BBC

ENGINEERING DIVISION

MONOGRAPH

NUMBER 50: **SEPTEMBER 1963**

New Methods of Lens Testing and Measurement

Part I

A PHOTO-ELECTRIC LENS TESTING BENCH

by

W. N. SPROSON, M.A., and K. HACKING, B.Sc.
(Research Department, BBC Engineering Division)

Part II

A METHOD OF OBSERVING AND RECORDING THE SOURCES OF FLARE IN A LENS

by

K. HACKING, B.Sc., and J. C. MARTIN
(Research Department, BBC Engineering Division)

BRITISH BROADCASTING CORPORATION

PRICE FIVE SHILLINGS

BBC ENGINEERING MONOGRAPH

No. 50

NEW METHODS OF LENS TESTING AND MEASUREMENT

Part I

A PHOTO-ELECTRIC LENS TESTING BENCH

by

W. N. SPROSON, M.A.

and

K. HACKING, B.Sc.

(Research Department, BBC Engineering Division)

Part II

A METHOD OF OBSERVING AND RECORDING THE SOURCES OF FLARE IN A LENS

by

K. HACKING, B.Sc.

and

J. C. MARTIN

(Research Department, BBC Engineering Division)

SEPTEMBER 1963

BRITISH BROADCASTING CORPORATION

FOREWORD

THIS is one of a series of Engineering Monographs published by the British Broadcasting Corporation. About six are produced every year, each dealing with a technical subject within the field of television and sound broadcasting. Each Monograph describes work that has been done by the Engineering Division of the BBC and includes, where appropriate, a survey of earlier work on the same subject. From time to time the series may include selected reprints of articles by BBC authors that have appeared in technical journals. Papers dealing with general engineering developments in broadcasting may also be included occasionally.

This series should be of interest and value to engineers engaged in the fields of broadcasting and of telecommunications generally.

Individual copies cost 5s. post free, while the annual subscription is £1 post free. Orders can be placed with newsagents and booksellers, or BBC publications, 35 MARYLEBONE HIGH STREET, LONDON, W.1.

CONTENTS

PREVIOUS ISSUES IN THIS SERIES

No.	Title	Date
1.	*The Suppressed Frame System of Telerecording*	JUNE 1955
2.	*Absolute Measurements in Magnetic Recording*	SEPTEMBER 1955
3.	*The Visibility of Noise in Television*	OCTOBER 1955
4.	*The Design of a Ribbon Type Pressure-gradient Microphone for Broadcast Transmission*	DECEMBER 1955
5.	*Reproducing Equipment for Fine-groove Records*	FEBRUARY 1956
6.	*A V.H.F./U.H.F. Field-strength Recording Receiver using Post-detector Selectivity*	APRIL 1956
7.	*The Design of a High Quality Commentator's Microphone Insensitive to Ambient Noise*	JUNE 1956
8.	*An Automatic Integrator for Determining the Mean Spherical Response of Loudspeakers and Microphones*	AUGUST 1956
9.	*The Application of Phase-coherent Detection and Correlation Methods to Room Acoustics*	NOVEMBER 1956
10.	*An Automatic System for Synchronizing Sound on Quarter-inch Magnetic Tape with Action on 35-mm Cinematograph Film*	JANUARY 1957
11.	*Engineering Training in the BBC*	MARCH 1957
12.	*An Improved 'Roving Eye'*	APRIL 1957
13.	*The BBC Riverside Television Studios: The Architectural Aspects*	JULY 1957
14.	*The BBC Riverside Television Studios: Some Aspects of Technical Planning and Equipment*	OCTOBER 1957
15.	*New Equipment and Methods for the Evaluation of the Performance of Lenses of Television*	DECEMBER 1957
16.	*Analysis and Measurement of Programme Levels*	MARCH 1958
17.	*The Design of a Linear Phase-shift Low-pass Filter*	APRIL 1958
18.	*The BBC Colour Television Tests: An Appraisal of Results*	MAY 1958
19.	*A U.H.F. Television Link for Outside Broadcasts*	JUNE 1958
20.	*The BBC's Mark II Mobile Studio and Control Room for the Sound Broadcasting Service*	AUGUST 1958
21.	*Two New BBC Transparancies for Testing Television Camera Channels (Out of Print)*	NOVEMBER 1958
22.	*The Engineering Facilities of the BBC Monitoring Service*	DECEMBER 1958
23.	*The Crystal Palace Band I Television Transmitting Aerial*	FEBRUARY 1959
24.	*The Measurement of Random Noise in the presence of a Television Signal*	MARCH 1959
25.	*A Quality-checking Receiver for V.H.F. F.M. Sound Broadcasting*	JUNE 1959
26.	*Transistor Amplifiers for Sound Broadcasting*	AUGUST 1959
27.	*The Equipment of the BBC Television Film Studios at Ealing*	JANUARY 1960
28.	*Programme Switching, Control, and Monitoring in Sound Broadcasting*	FEBRUARY 1960
29.	*A Summary of the Present Position of Stereophonic Broadcasting*	APRIL 1960
30.	*Film Processing and After-processing Treatment of 16-mm Films*	MAY 1960
31.	*The Power Gain of Multi-tiered V.H.F. Transmitting Aerials*	JULY 1960
32.	*A New Survey of the BBC Experimental Colour Transmissions*	OCTOBER 1960
33.	*Sensitometric Control in Film Making*	DECEMBER 1960
34.	*A Mobile Laboratory for UHF and VHF Television Surveys*	FEBRUARY 1961
35.	*Tables of Horizontal Radiation Patterns of Dipoles Mounted on Cylinders*	FEBRUARY 1961
36.	*Some Aspects of Optical Lens Performance*	APRIL 1961
37.	*An Instrument for Measuring Television Signal-to-noise Ratio*	JUNE 1961
38.	*Operational Research on Microphone and Studio Techniques in Stereophony*	SEPTEMBER 1961
39.	*Twenty-five Years of BBC Television*	OCTOBER 1961
40.	*The Broadcasting of Music in Television*	FEBRUARY 1962
41.	*The Design of a Group of Plug-in Television Studio Amplifiers*	APRIL 1962
42.	*Apparatus for Television and Sound Relay Stations*	JULY 1962
43.	*Propagational Factors in Short-wave Broadcasting*	AUGUST 1962
44.	*A Band V Signal-frequency and a Correlation Detector for a VHF/UHF Field-strength Recording Receiver*	OCTOBER 1962
45.	*Vertical Resolution and Line Broadening*	DECEMBER 1962
46.	*The Application of Transistors to Sound Broadcasting*	FEBRUARY 1963
47.	*Vertical Aperture Correction using Continuously Variable Ultrasonic Delay Lines*	MAY 1963
48.	*The Development of BBC Internal Telecommunications*	MAY 1963
49.	*Apparatus for Measurement of Non-linear Distortion as a Continuous Function of Frequency*	JULY 1963

NEW METHODS OF LENS TESTING AND MEASUREMENT

SUMMARY

Part I of this monograph describes a photo-electric lens test bench capable of measuring lenses of focal length from 12 mm to 1 m. Designed specifically for television applications, it gives the 'optical transfer' curve automatically plotted on recording paper, using the sine-wave analyser described by Hacking. Facility is also provided for the recording of the 'spread function'. The angular field is somewhat in excess of $\pm 45°$: the field diagonal in the image plane is limited to $\pm$ 100 mm. An air-spaced doublet of 3·05 m focal length and 200 mm diameter is used as collimator.

Provision is made for the measurement of the optical transfer function for imagery at finite conjugates by the addition of a second cross-slide with its own light source and test object. The bench is physically large enough to accommodate large zoom lenses and complete optical systems.

Some comparisons of two basic types of optical bench are given and the accuracy of the final result is discussed.

Part II deals with an optical arrangement which can be used to examine a lens, by visual means, for surface defects (e.g. dust, scratches, poor blooming, etc.). This type of defect gives rise to flare and loss of contrast in the image formed by the lens. In the visual field of the device the sources of flare in the lens are seen as points or patches of light against a dark background. Thus the method is similar to the dark-ground illumination technique used in microscopy. Photographs of the flare-source patterns obtained from several camera and enlarging lenses are shown. These serve to illustrate some common flare-producing defects.

PART I

A PHOTOELECTRIC LENS TESTING BENCH

1. Introduction

The optical bench was designed and constructed so that accurate measurement of the modulation transfer characteristic of any lens likely to be used by the Television Service could be made. Prior to the installation of this bench in January 1960, measurements of modulation transfer characteristics were made on a modified version of the Mark 1 Taylor Hobson Optical Bench.[1] A serious limitation of this bench was its inability to measure lenses of focal length in excess of 6 in. (150 mm). Further, the measurement of lenses at finite conjugates was not easy with this particular bench as it was intended primarily for working with a test object at infinity.

In designing a new and larger optical bench, it was desirable that these two limitations should be overcome and the attempt was made to design a bench suitable for all optical measurements (of modulation transfer characteristic) relevant to television. These include complete optical systems and zoom lenses in addition to fixed-focus single lenses.

2. Requirements

2.1. *For Single Lenses*

Focal length range:	from $\frac{1}{2}$ in. to 40 in. (12·7 to 1016 mm)
Aperture:	f/1·0 to f/16
Semi-angular field:	not less than 40°
Spatial frequencies:	normally from zero up to about 30 c/mm (occasionally up to 60 c/mm)
Object distance:	either infinite or finite as application demands

2.2. *For Zoom Lenses*

In addition to measuring the modulation transfer characteristic for a range of focal lengths from 12 mm to 1 m, the minimum working distance for accurate zooming should be easy to check.

2.3. *For Optical Systems*

Sufficient space should be available to install and measure complete systems such as colour-camera optical systems and multiplex telecine optics.

3. Methods of Measurement of the Optical Transfer Function*

Prior to 1960, the standard method of determining the optical transfer function in the BBC Research Department was by means of the 'spread function'. This was recorded automatically[2] and a Fourier transform of the spread function was obtained by a sampling method using a desk-calculator.[3] This method was adequate for our purposes but suffered one grave disadvantage, namely that the process of sampling the spread function and then doing the computation on the desk-calculator was very time-consuming.

In 1958, Hacking[4] suggested a method, based on an optical Fourier transform generator originally described by Born *et al*,[5] in which the Fourier transform is obtained

* Optical transfer function is the name recommended by the International Commission for Optics for frequency response when both phase and amplitude are considered. The modulus of this is to be called 'modulation transfer function'.

directly from the spread function. It was decided that the new optical bench should provide for the use of this method as well as the older method.

4. Sine-wave Analyser

It may be appropriate at this point to explain how the sine-wave analyser performs the Fourier transform of the spread function. The lens under test forms an image of a thin slit test-object and this image is magnified by a microscope objective. The magnified image is made coplanar with a thin slit which is oriented at right angles to the image of the test-object slit. The thin slit thus takes a representative sample of the magnified image. Immediately behind this thin slit is a photographic plate which has a sinusoidal variation of transmission (sine-wave grating). The spread function is thus multiplied by a sinusoid and the transmitted light flux is then allowed to fall on the photocathode of a photomultiplier where integration takes place, the current flowing in the photomultiplier being directly proportional to

$$\int_{-A}^{A} f(x)\cos(\omega x + \delta)\,dx + C$$

where $f(x)$ is the spread function

$\omega/2\pi$ is the spatial frequency of the sinusoid (as seen through the thin slit)

δ is an arbitrary phase angle depending on the setting of the sinusoid vis-a-vis $f(x)$

$2A$ is the length of the thin slit (near to the sinusoid)

C is a constant depending on the mean transmission of the sine-wave plate.

The spatial frequency $\omega/2\pi$ can be changed by causing the sine-wave plate to rotate. If the lines of constant transmission are initially parallel to the thin slit, the effective spatial frequency will be zero; when the lines of constant transmission are perpendicular to the thin slit, then the spatial frequency will be a maximum (f_0) and for intermediate values of rotational angle θ we have

$$f = f_0 \sin\theta$$

In the mechanical drive of the sine-wave plate, a mechanical coupling (Fig. 1) is used so that the frequency scale on the recording paper shall be linear rather than one depending on the sine of the angle of rotation. In the present equipment a rotation of 70° is employed. This gives over 90 per cent of the maximum possible frequency range of the sine-wave plate.

Two settings of the phase of the sine-wave plate with reference to the adjacent thin slit are usually necessary for the complete Fourier transform; the cosine component* is obtained with the sine-wave plate adjusted to obtain the maximum photocurrent. It may be shown that the sine component is obtained by a lateral shift of the sine-wave plate such that the photocurrent corresponds to the mean transmission of the sine-wave plate at zero spatial frequency. It is essential that as the sine-wave plate rotates, a constant phase position (e.g. a maximum) be maintained

* The sine and cosine components are only one special case of the two components required for a Fourier transform. Any two components which have a 90° phase shift will suffice.

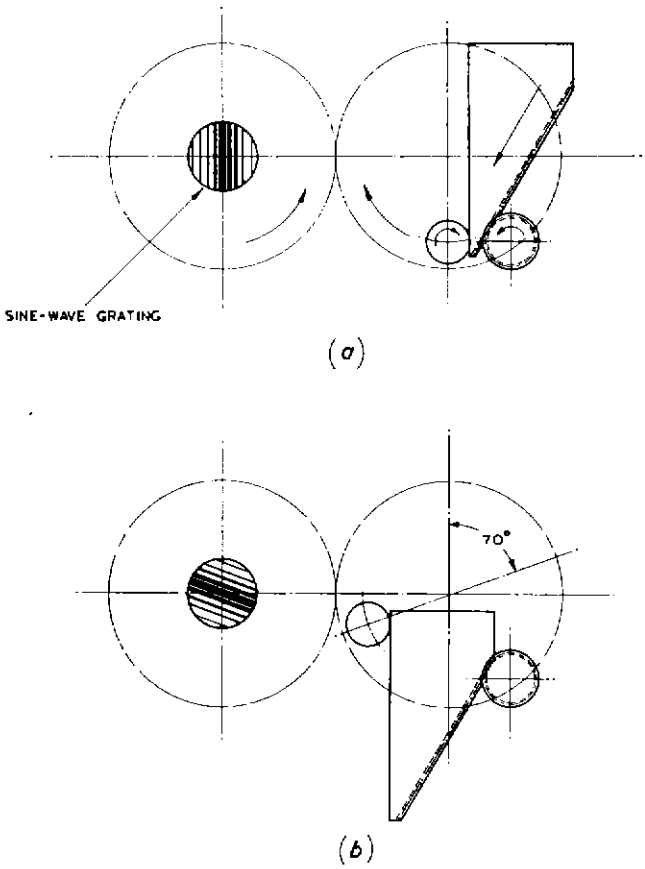

Fig. 1 — Mechanical coupling used with sine-wave analyser

(a) *Beginning of the recording cycle*
(b) *End of the recording cycle*

at the centre of the slit. The mathematical process involved in these two operations is illustrated in Figs. 2(a) and 2(b). The only difference between the mathematical process and the method used in the sine-wave analyser arises because the sinusoidal plate has a non-zero mean level, but this is trivial and can easily be allowed for. The modulus of the optical-transfer function is the root sum of the squares of the sine and cosine components.

5. Basic Design

The optical bench used up to 1960 was an adaptation of a Mark 1 Taylor Hobson Bench[1] and was of the nodal-slide type. This means that the lens is mounted on a turntable and adjustment is provided so that the rear nodal point of the lens under test can be brought into coincidence with the axis of rotation of the turntable. Under these conditions the image suffers no lateral movement when the turntable is rotated. The provision of a tee-bar makes automatic adjustment for the increase in back-working-distance for off-axis imagery. Figs. 3(a) and 3(b) show diagrammatically the operation of this type of bench.

Another type of optical bench may be called the

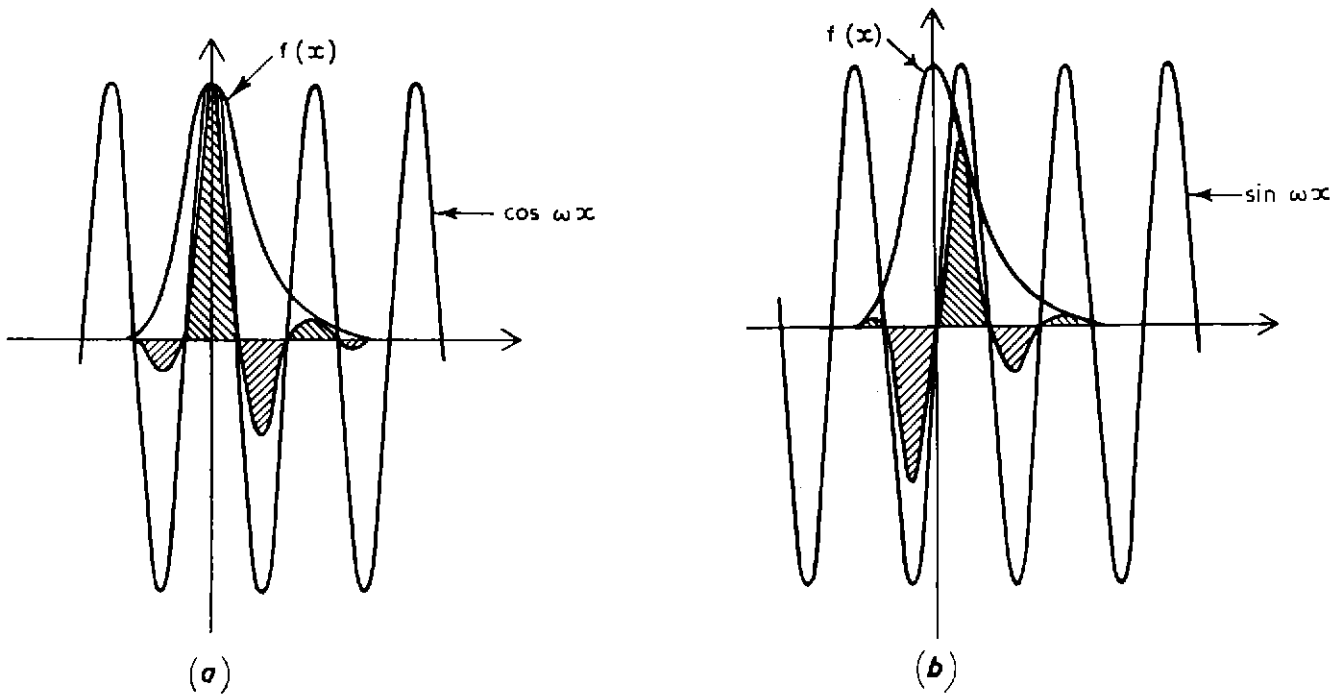

Fig. 2 — Illustrating the cosine and sine components of a Fourier transform

(a) *Cosine component* $\int f(x) \cos \omega x.\, dx$ *is the sum of the shaded area (due regard being paid to sign)*

(b) *Sine component* $\int f(x) \sin \omega x.\, dx$ *is the sum of the shaded areas (due regard being paid to sign)*

swinging-arm bench; an example of this type was exhibited by Messrs Precision Tool and Instrument Company at the 1956 Annual Exhibition of the Physical Society. This bench was of large dimensions and appeared to satisfy many of the requirements listed in Section 2. The mode of operation of a swinging-arm bench is illustrated in Figs. 4(a) and 4(b).

Before deciding whether to continue using a nodal-slide type of bench (but clearly of much larger dimensions than the Mark 1 Taylor Hobson bench) or to use the swinging-arm type, it was necessary to consider the advantages and disadvantages of each type.

The advantages of a nodal-slide type of bench can be summarized as follows:

(i) the image remains located substantially in one position;
(ii) direct measurement of focal length is possible;
(iii) determination of geometrical distortion is straightforward.

The disadvantages are:

(i) rotation about the rear nodal point can cause the front element of a long lens to swing out of the beam of the collimator;
(ii) the bench is not easily adapted for measurements at finite conjugates;
(iii) the bench is less adaptable for measurement of complete optical systems.

The swinging-arm type of bench has the following advantages:

(i) rotation of front element can easily be arranged to coincide with the axis of the swinging arm; hence the front element of the lens under test never swings out of the beam of the collimator and uses substantially the same portion of the beam given by the collimator for axial and off-axis measurements.
(ii) basic simplicity of design means easy adaptation for finite-conjugate working and also testing complete optical systems.

The disadvantages are:

(i) off-axis image has to be located and hence a rapid visual inspection of the whole field is not possible;
(ii) focal length is not directly given;
(iii) geometrical distortion not easily measured.

In view of its greater versatility it was decided to use a swinging-arm type of bench for the new optical bench, although clearly each type of bench has its own particular virtues.

6. Detailed Description of the Optical Bench

An overall view of the bench is given in Fig. 5. The light source A is a 100-watt tungsten lamp together with a condenser and one sheet of diffusing material. Provision is

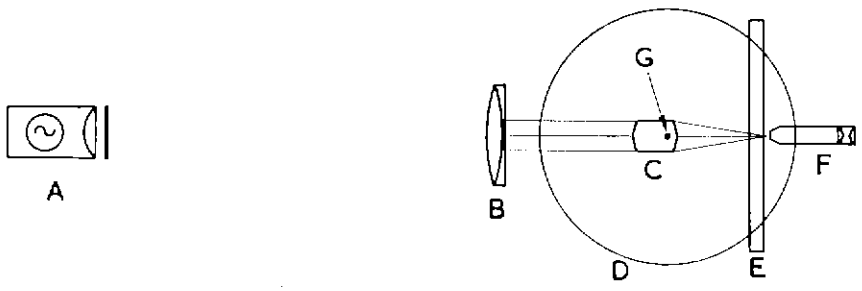

(a) Axial setting

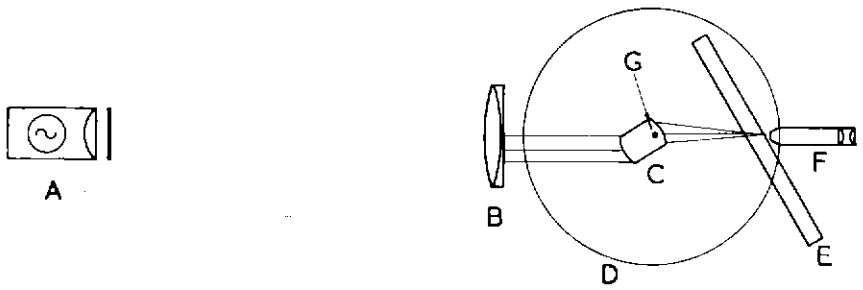

(b) Off-axis setting

Fig. 3 — Nodal-slide optical bench

A *Light source and test object*
B *Collimator*
C *Lens under test*
D *Nodal slide turntable*
E *Tee-Bar*
F *Viewing and detecting system*
G *Axis of rotation of slide turntable (coincident with rear nodal point of lens)*

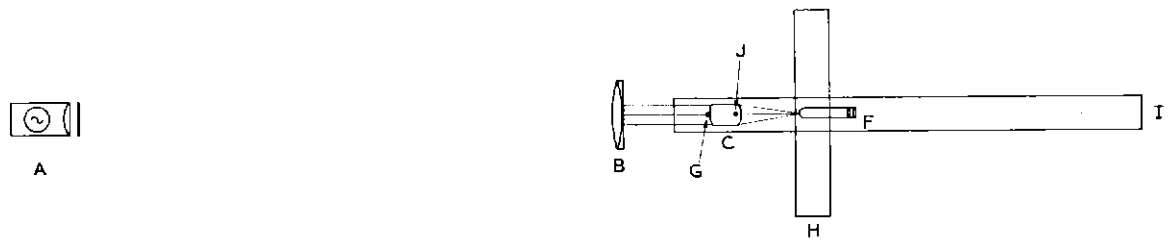

(a) Axial setting

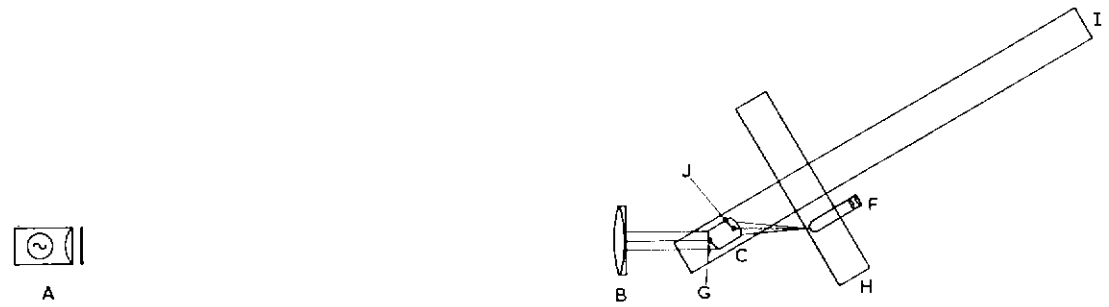

(b) Off-axis setting

Fig. 4 — Swinging-arm optical bench

A *Light source and test object*
B *Collimator*
C *Lens under test*
F *Viewing and detecting system*
G *Axis of rotation of swinging-arm*
H *Cross-slide*
I *Swing-arm*
J *Rear nodal point of lens*

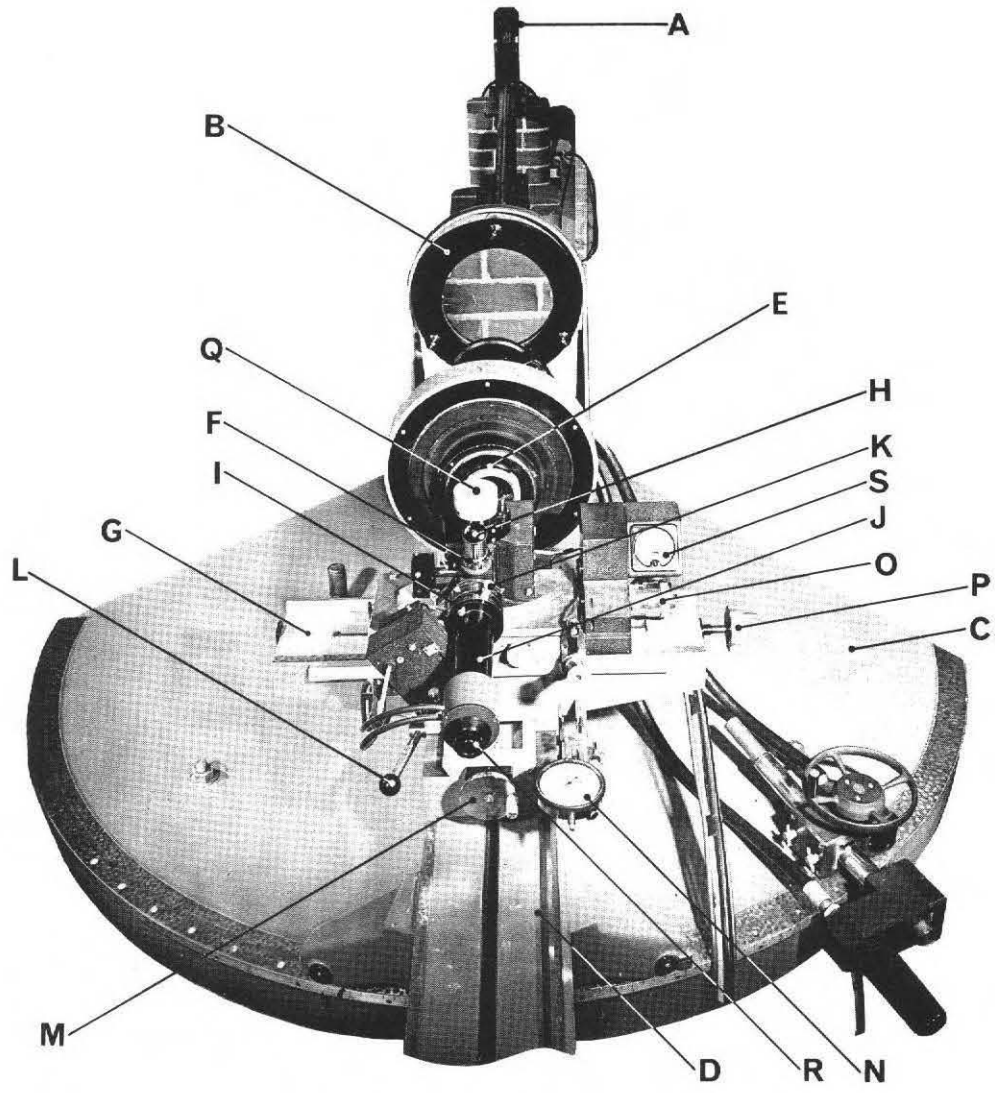

Fig. 5 — Photograph of optical bench

made for the insertion of neutral filters and colour filters behind the test object which usually takes the form of a thin slit. The lamp house is mounted on a two metre optical bench of triangular cross-section. For measurements at infinite conjugate, the test object is positioned at the focus of the 120 in. (3·05 m) collimator lens B which is an air-spaced doublet of 8 in. (20 cm) diameter. The collimator can be removed by unscrewing the three knurled screws whereupon axial measurements at finite conjugates can be made.*

The collimator bracket is mounted on a large sector-shaped horizontal casting C which carries the swinging arm D upon which is mounted the lens under test E and the image-viewing and measuring device F, the latter being mounted on the cross slide G. The lens under test forms an image of the test object slit which is magnified by a relay lens (8 mm and 4 mm apochromatic microscope objectives are used for this purpose). The magnified image can be viewed through the eyepiece H or measured by means of the sine-wave analyser I and photomultiplier photocell J. The knob K (which is more clearly seen in Fig. 6) controls the phase of the sine-wave plate.

The knob L controls a locking device on the carriage supporting the cross-slide G and coarse focusing is achieved by moving the whole assembly along the sliding arm D. Fine focusing is achieved by rotating the knob M which rotates a micrometer screw of 40 t.p.i. Shifts of focus can be read-off on the dial gauge N which is graduated in intervals of 10μ and can be estimated to about 2μ. Centr-

* Off-axis measurements at finite conjugates require the use of either a second cross-slide not shown in Fig. 5 or a manual adjustment of the light source distance for each field angle [$\Delta = (1 + m)(\sec\theta - 1)f$] · where Δ = change in distance of test object, f is the focal length, m = magnification, and θ = field angle.

ing of the image can be done either by the micrometer O, or the wheel P. The reason for two adjustments is that the micrometer O is driven by an impulse motor when making a recording of a tangential spread function and it is usually convenient to use this for small lateral shifts. The wheel P is used for larger shifts of the image receiving system which are necessary when an off-axis image is being found. Vertical centring of the image is available by rotating Q, which lifts the microscope tube, sine-wave analyser, and photocell. The photomultiplier output is fed to an amplifier via the potentiometer R. The output from the amplifier operates the recording milliammeter and also the meter S (in series with the recorder) which is conveniently placed for reading during the setting-up of the lens under test.

A more detailed view of the receiving and viewing system is shown in Fig. 6. The impulse motor T is used when a tangential spread function is required, as stated above. This drives the micrometer O in steps of 1 μ through a gear-train so that a slow mechanical scanning of the image is performed. For this purpose, the slit in the sine-wave analyser is made parallel to the vertical test object slit. The vertical centring knob Q can also be driven by an impulse motor U so that a sagittal spread function can be recorded. The test object slit and the sine-wave slit are both rotated to a horizontal setting for a sagittal spread function. As with the automatic recording facility on the Taylor Hobson bench,[1] three rates of recording of spread function are available viz. 10, 20, and 40 microns per inch of recording paper.

For off-axis measurements when the swinging arm is inclined at a large angle to the optical axis of the collimator, it is necessary to rotate the image receiving system (consisting of microscope objective, sine-wave analyser, and photo-multiplier) if the microscope objective is not to restrict the image-forming rays. Facility for doing this is provided by pivoting the sector-shaped plate which supports the image receiving system on a vertical axis a little in front of the front edge of the cross-slide G. The sector-shaped plate is clamped by the small lever V. As an example of the angular field covered without the need to use this facility, a lens with a relative aperture of $f/2$ can be tested up to 30° semi-angular field. Beyond 30° the image receiving system must be rotated towards the incoming light rays.

The output from the photomultiplier is insufficient to operate the recording milliammeter so that a current amplifier with a gain of the order of 10^3 is required. A valve amplifier was used with the Taylor Hobson bench: the corresponding unit in the new optical bench is a transistor amplifier. As a result of this change there has been a

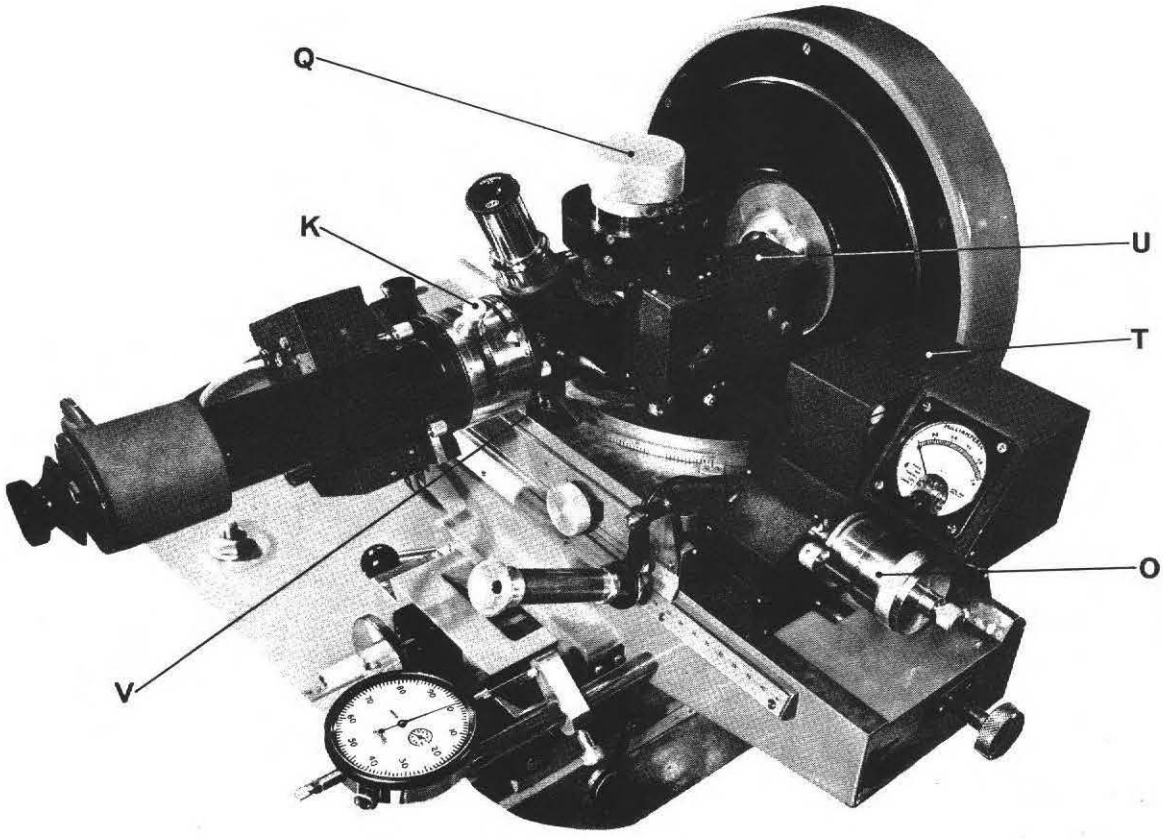

Fig. 6 — Scanning head, sine-wave analyser, and cross-slide of optical bench

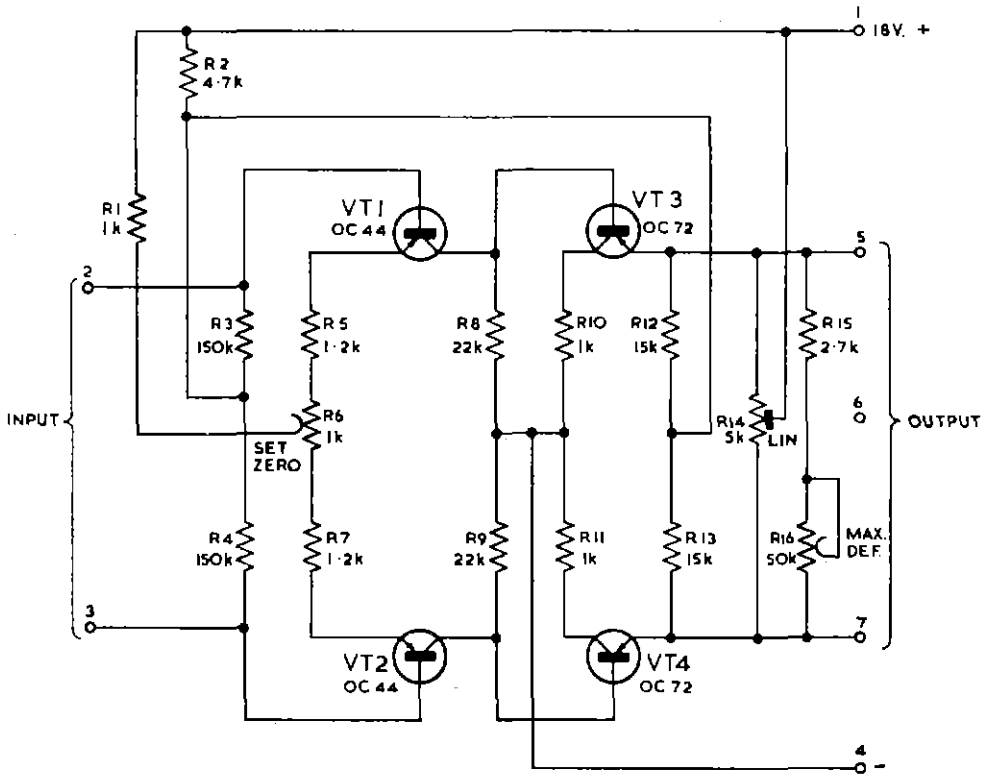

Fig. 7 — Circuit diagram of current amplifier

marked improvement in the stability of the black level. The amplifier is battery-operated with Mallory mercury cells; its circuit diagram is given in Fig. 7.

A point of interest arises in the application of aperture correction for the finite width of the object and scanning slits. In the spread function method, the corrections for both object and scanning slit are in the same sense, i.e. both slits are responsible for a loss of modulation at the higher spatial frequencies. In the case of the sine-wave analyser,* the two corrections are in opposite senses and this makes it possible to achieve a direct result which requires virtually no aperture correction. The mathematical form of the two corrections is not identical, but if the nominal width of the image of the test object slit is made equal to the width of the slit in the sine-wave analyser (as seen through the microscope objective) and provided that this width is less than a quarter of the shortest wavelength tested, then the corrections are self-cancelling to better than half a per cent over the range of spatial frequencies investigated.

7. Measurements at Finite Conjugates

A second cross-slide is used when measurements are required at finite conjugates. This cross-slide has its own light source. The same slit assembly is used for working at either infinite or finite conjugates. This assembly has nine slits any of which can be brought to the central, active, position: it is also easy to rotate the slits so that they are either vertical (for tangential modulation transfer functions) or horizontal (for sagittal functions).* The slits were prepared by vacuum evaporation of aluminium on to a glass plate with a wire of appropriate diameter stretched across the glass (and in contact with it). The widths of the slits range from $13\frac{1}{2}$ to 1226μ. This range is needed so that the nominal image produced by the lens under test shall be about 5μ. Even so, the range is not as great as would be desirable, e.g. for measurements at unity magnification a slit of 5μ would be highly desirable. The present practice is to make the necessary aperture correction when the nominal image of the object slit is not 5μ.

The light housing on the cross slide is arranged to rotate about a vertical axis through the object slit. This was found to be vital for off-axis working; otherwise little or no light flux from the object slit reaches the entrance pupil of the lens under test.

* For a mathematical treatment, see the Appendix.

8. Performance Tests

8.1. *Sine-wave Analyser*

There are a number of features of the sine-wave analyser which require accurate construction and careful checking

* The measurement of the spread function is limited to tangential and sagittal orientations of the test object. The sine-wave analyser, however, is not restricted to these two orientations since it suffices for the analyser slit to be orthogonal to the test object slit, and the sine-wave plate can be rotated so that it is parallel to the analyser slit at the commencement of a recording.

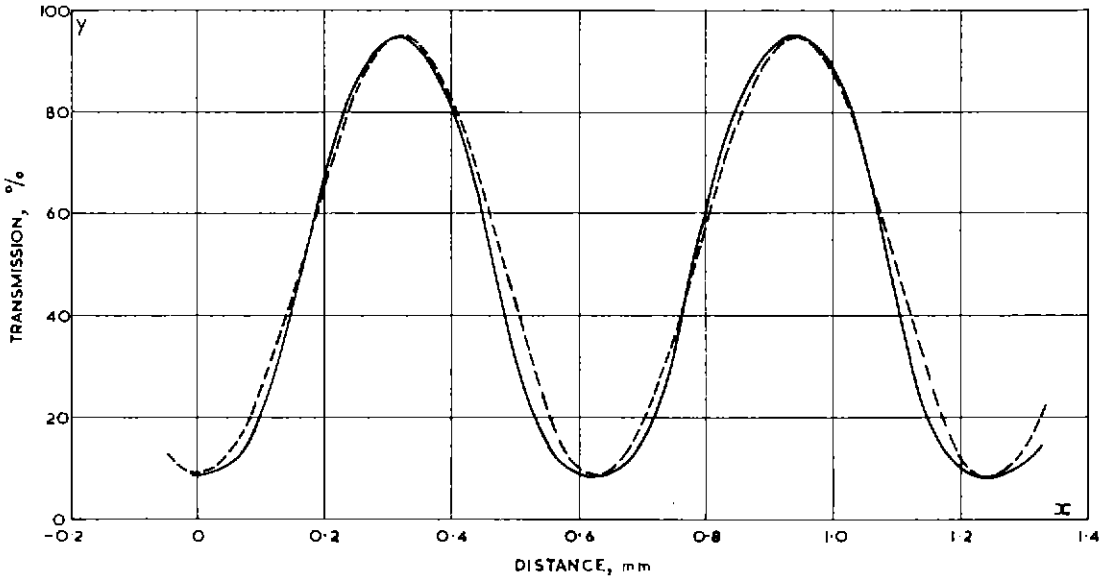

Fig. 8 — Transmission characteristic of the sine-wave grating

——— *Measurement*

– – – – – *Plot of* $y = 52 + 43 \sin 2\pi \left(\frac{x - 0{\cdot}164}{0{\cdot}618}\right)$

in order that the results shall be reliable. The concentricity of rotation of the sine-wave plate needs to be good: some relaxation in mechanical tolerances is obtained by virtue of the fact that the sinusoid is situated in the magnified image plane. If we take 30 c/mm in the primary image plane as the highest spatial frequency measured (in conjunction with an 8 mm apochromatic relay lens), then the smallest wavelength is 33μ, which becomes 660μ in the magnified image plane. Any error of centring should certainly be less than one-tenth of this figure and preferably better than one-twentieth. Examination of this part of the apparatus shows a maximum shift of the order of about 10μ which is small in terms of the minimum wavelength used.

Another feature of the sine-wave analyser which is essential for accurate results is the correct transmission characteristic of the sine-wave plate. The sine-wave plate was made by an interference technique. Localized fringes formed by a thin wedge in monochromatic light (green 5461 Å Hg line isolated by an Ilford Mercury filter) were photographed and a positive was printed from the negative. The transmission characteristic is shown in Fig. 8. A compromise needs to be effected between the contrast (modulation depth) and accuracy of characteristic. In order to obtain a high contrast a considerable excursion of the photographic transfer curve ('H and D' curve) is used and non-linearity becomes increasingly troublesome: hence a good approximation to a sine-wave is difficult to achieve with high contrast. In the present case, a modulation of about 84 per cent is obtained with a fair approximation to a sine-wave transmission characteristic.

Probably the best way of checking the performance of the sine-wave analyser is to present it with a function (i.e. test object) whose Fourier transform is well known and precisely determined. A slit uniformly illuminated with incoherent light satisfies this requirement and its normalized Fourier transform is the $(\sin kv)/kv$ function, where v is the spatial frequency and k is $2\pi b$ for a slit of width $2b$. Two examples of this are given in Fig. 9 where the continuous curves are the mathematical $(\sin kv)/kv$ functions and the plot points are the measured values. This check serves two purposes, (i) it shows whether the spatial frequency scale (abscissa) is correct by virtue of the location of the zeros; (ii) it checks the shape of the output curve which is dependent mainly on the accuracy of form of the sine-wave plate. Check (i) is independent of check (ii).

8.2. *Comparison of Sine-wave Analyser Results with Results obtained by the Spread Function Method*

This comparison is most easily shown in graphical form and Figs. 10, 11, and 12 are offered in evidence of the substantial agreement which has been achieved between the two methods. Figs. 10 and 11 relate to axial modulation transfer functions and Fig. 12 relates to an off-axis function. In the case of an image whose spread function is very extensive, the sine-wave analyser can give a slightly favourable answer because its slit has a finite length and the spread-function may extend beyond this. This fact is responsible for the greater modulation transfer factor in the range of spatial frequencies from 0 to 12 c/mm (Fig. 12) when the sine-wave analyser results are compared with those derived from the spread function. This limitation of the sine-wave analyser applies only in cases where the quality of the image is relatively poor and well below the standard laid down in the BBC Specification for lenses.[6]

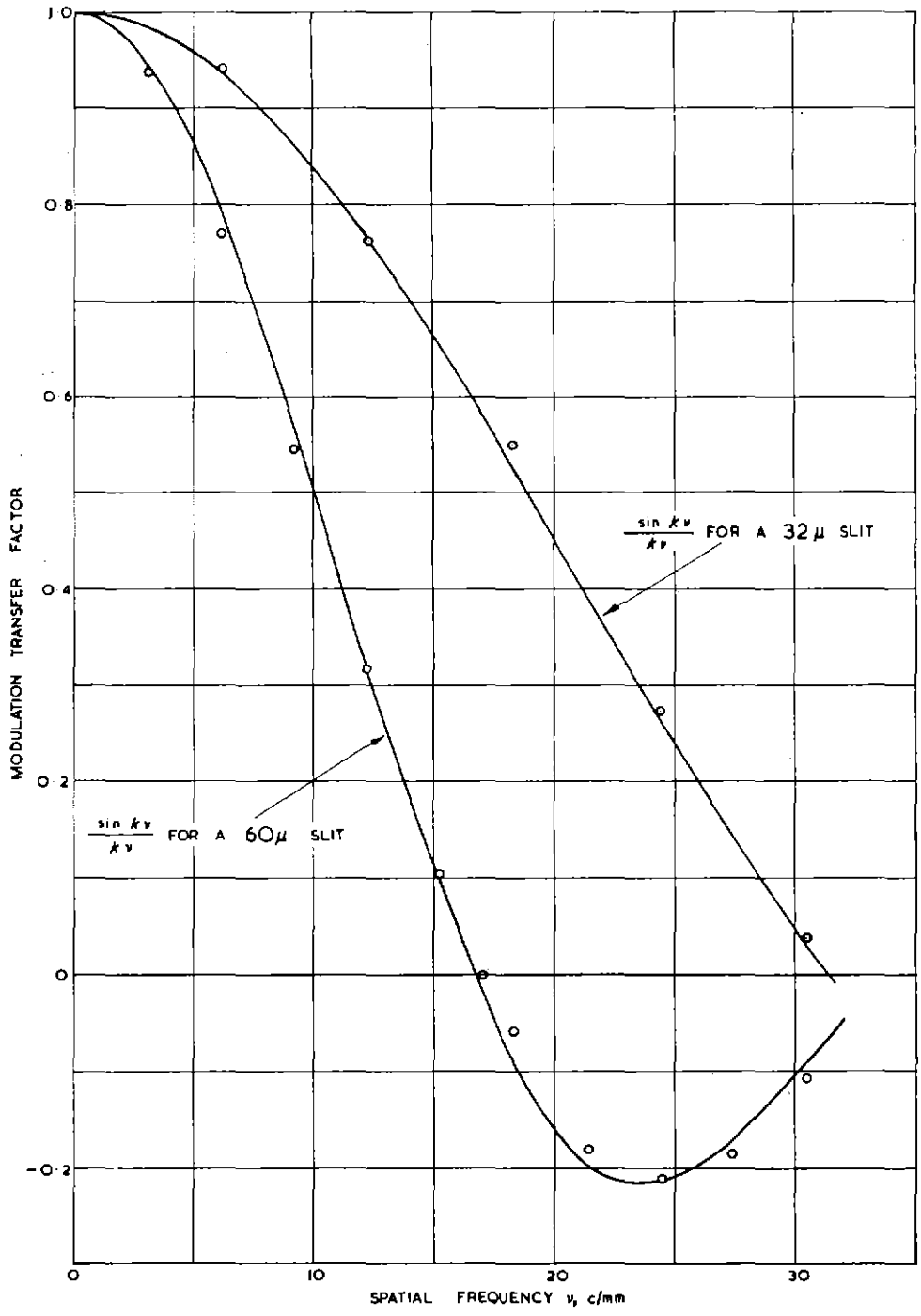

Fig. 9 — Comparison of theoretical and practical results for two rectangular slits

$k = 2\pi b$, *where* $2b$ = *width of slit*
o o o *Experimental results*
——— *Theoretical results*

The results given in Figs. 10 and 11 show that the two methods give results which never disagree by more than 3 per cent over the range of spatial frequencies from zero to 30 cycles per mm.

8.3. *Modulation Transfer Function of the Microscope Objective*

The primary image formed by the lens under test is relayed by a microscope objective on to the plane of the

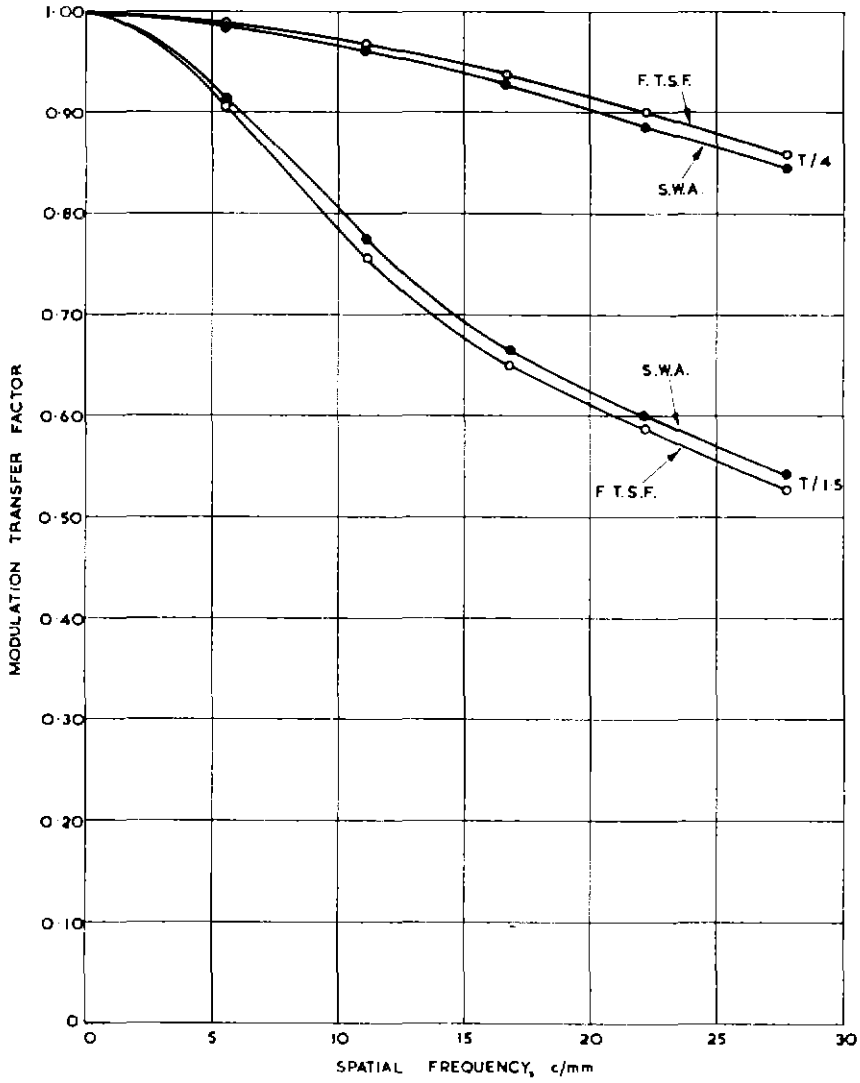

Fig. 10 — Comparison of results for a 5 cm T/1·5 lens: axial image

o——o *Fourier transform of spread function*
●——● *Sine-wave analyser*

slit. It is essential that the microscope objective shall make a negligible contribution to the aberrations of the lens under test. The modulation transfer function of the 8 mm apochromat used as a relay lens was measured by determining the spread function produced by a 5μ slit when imaged by the objective (this measurement was done on the Mark 1 TTH bench). The result is shown in Fig. 13 and it will be observed that up to 30 c/mm the loss in modulation is less than 2 per cent.

In Section 8.1 the test using a slit includes any errors introduced by the microscope relay lens.

8.4. *Consistency of Measurements using the Sine-wave Analyser*

The measurements given in Section 8.2 were done by one careful observer. It is of interest to know whether measurements are repeatable and whether different workers obtain the same result. To answer the latter question, the modulation transfer function of a defocused 50 mm lens was measured by four workers. The reason for choosing a defocused image is that a steeply descending function is more sensitive to positional experimental errors in the frequency scale than a monotonic function of high value throughout the range of measurements. The results are given in Table 1.

It will be observed that the maximum standard deviation is about 2 per cent and this holds over the range of spatial frequencies from 6 to 12 c/mm where the function is steeply descending (Fig. 14). It is considered that this represents the upper limit of inaccuracy of measurement (except for the case illustrated in Fig. 12 where the spread function exceeds the aperture of the slit in the sine-wave

TABLE I

SPATIAL FREQUENCY c/mm	MODULATION TRANSFER FACTOR % Worker 1	2	3	4	MEAN VALUE	DIFFERENCES FROM MEAN % Worker 1	2	3	4	STANDARD* DEVIATION %
3·05	95·7	94·6	93·5	92·4	94·05	1·65	0·55	−0·55	−1·65	1·42
6·1	77·4	76·4	76·1	73·0	75·72	1·68	0·68	0·38	−2·72	1·90
9·15	53·6	52·6	52·2	49·1	51·88	1·72	0·72	0·32	−2·78	1·94
12·2	31·6	30·5	28·5	27·1	29·42	2·18	1·08	−0·92	−2·32	2·01
15·25	13·2	13·5	12·6	10·4	12·42	0·78	1·08	0·18	−2·02	1·40
18·3	4·3	4·3	5·8	4·8	4·8	−0·5	−0·5	1·0	0	0·71

* Standard deviation σ is strictly $[\Sigma(\Delta x)^2/(n)]^{\frac{1}{2}}$: however, when n is small a better estimate of the standard deviation of the parent population is given by $[\Sigma(\Delta x)^2/(n-1)]^{\frac{1}{2}}$ and this formula has been used here. The standard deviation of the mean (standard error) is $\sigma/(n)^{\frac{1}{2}}$ which is half the value quoted in the last column for $n = 4$.

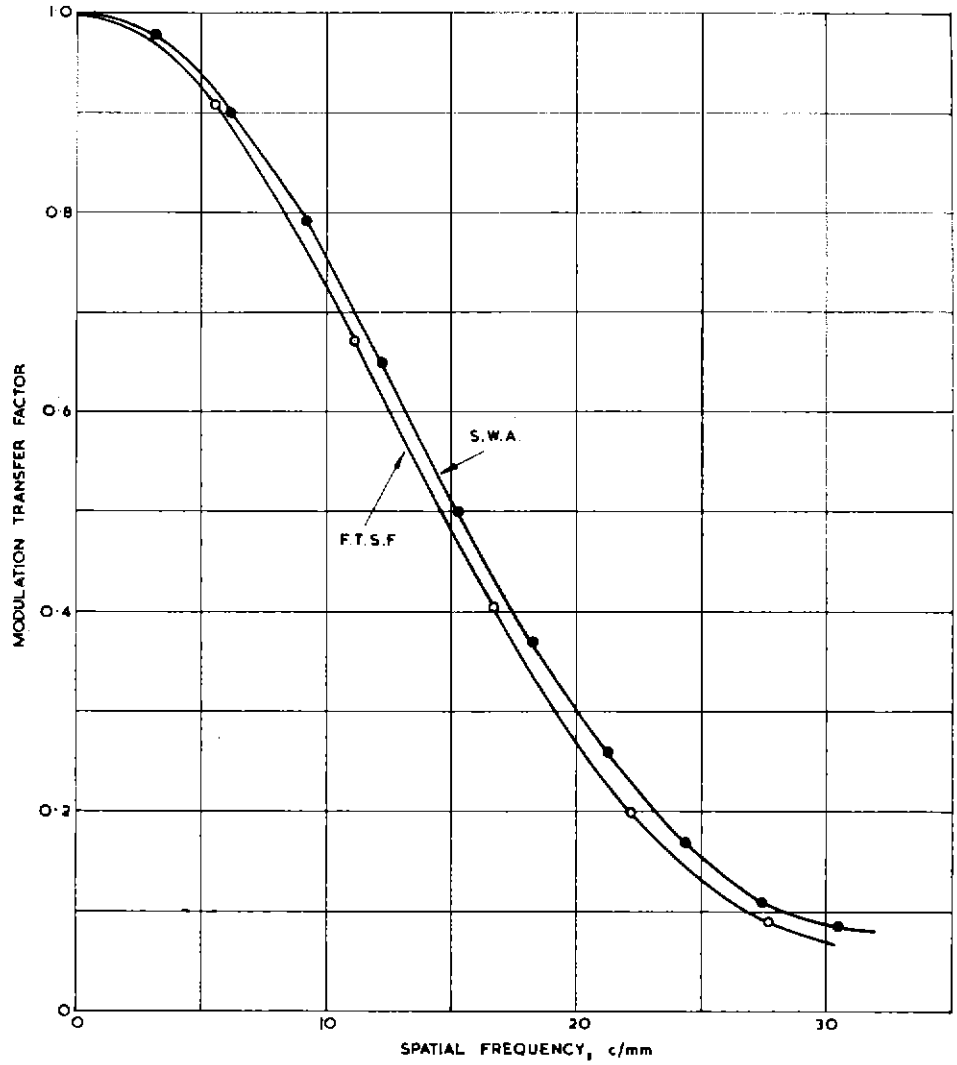

Fig. 11 — Comparison of results for a defocused 1½ in. (38 mm) f/1·9 lens: axial image

o——o *Fourier transform of spread function*

●——● *Sine-wave analyser*

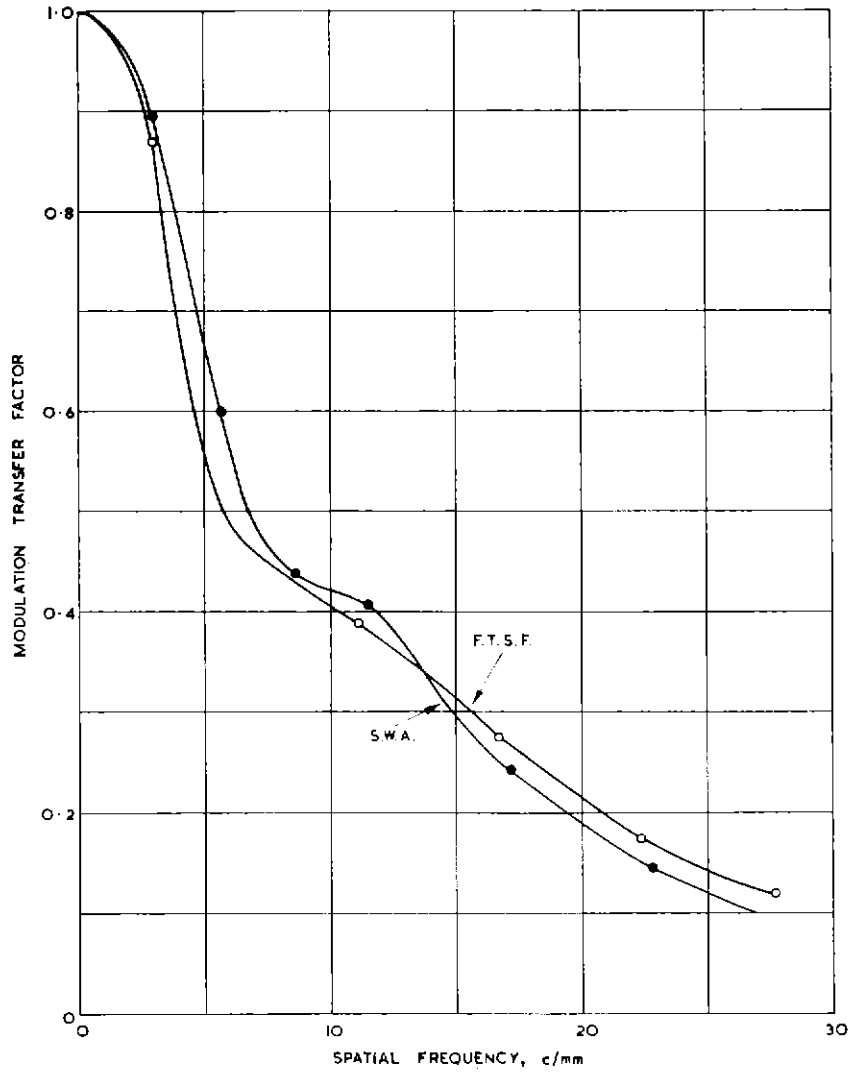

Fig. 12 — *Comparison of results of* $1\frac{1}{2}$ *in.* (38 *mm*) *f*/1·9 *lens at* 20° *tangential*

o——o *Fourier transform of spread function*
●——● *Sine-wave analyser*

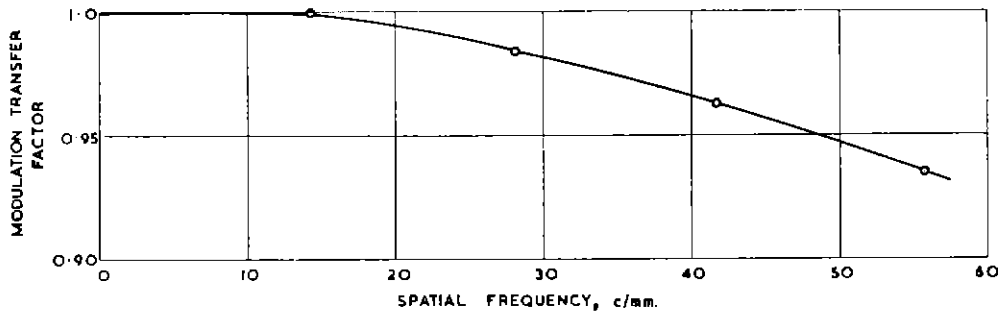

Fig. 13 — *Modulation transfer curve of the* 8 *mm apochromatic objective*

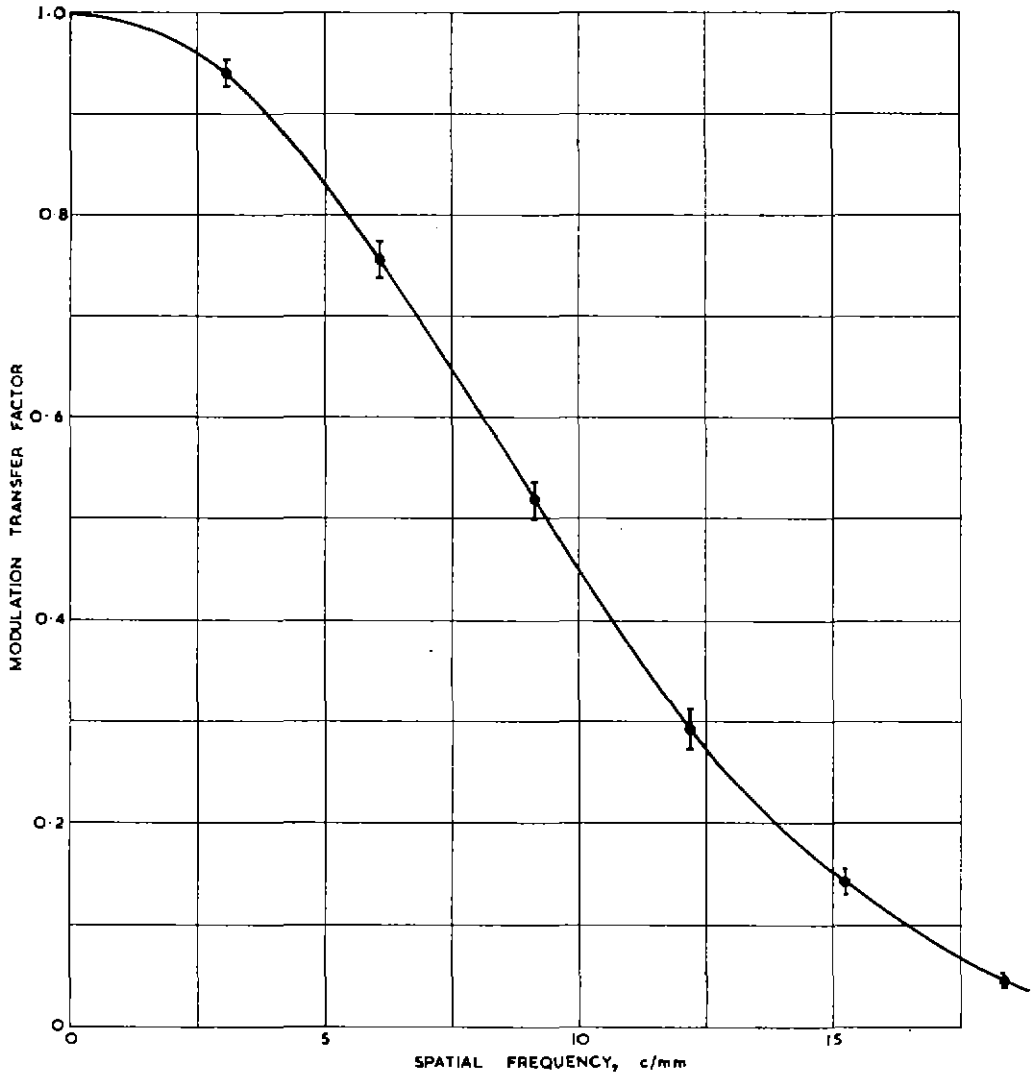

Fig. 14 — Consistency of results from four observers

Solid line is the mean. Vertical lines at plot points show ± standard deviation

analyser). This level of accuracy is considered sufficient for most purposes: an improvement can be effected if several measurements are taken and averaged but this is not normally necessary.

9. Operational Experience

The optical bench has now been in use for about two years. During this period a considerable number of lenses and optical systems have been measured. In the matter of fixed focus lenses, the shortest focal length encountered has been that of a 12 mm lens for 8 mm cinematography and the longest, that of a 40 in. (1·02 m) lens used with the image orthicon camera. The lens with the greatest angular field has been a 28 mm *f*/2 lens designed for the image orthicon camera (semi-angular field = 35° 6′). The largest zoom lens, which also uses folded optics in the rear conjugate axis was a five-to-one zoom lens designed for the image orthicon camera. Other zoom lenses include several with four-to-one zoom ratio and more recently two ten-to-one zoom lenses. So far no lens has been either too large or too small to be mounted and measured.

Multiplex optical systems for vidicon telecine machines and the optical systems of two colour cameras have been accommodated and measurements of the modulation transfer functions have been made. Sufficient space exists for the mounting of these systems and a blank saddle with a plane horizontal top surface has been very useful for mounting these systems with the aid of specially constructed units.

The facility for measurement at finite conjugates has been frequently used and is certainly very valuable in assessing lenses for flying-spot scanners and telerecording film cameras.

10. Conclusions

Facilities now exist for the fairly rapid measurement of the optical transfer function of all the lenses and optical systems likely to be employed in television. Up to a spatial frequency of 30 c/mm, the standard deviation of the measurements is of the order of 2 per cent. Measurement at finite conjugates can be accomplished with equal facility to those at infinite conjugates. The bench is sufficiently large and versatile to enable complete optical systems to be measured. It is doubtful whether a nodal-slide type of bench would have been suitable for all the lenses and optical systems which have been measured; the choice of a swinging-arm bench appears to have been completely justified.

PART II

A METHOD OF OBSERVING AND RECORDING THE SOURCES OF FLARE IN A LENS

11. Introduction

A photoelectric method of measuring the total amount of veiling-glare produced by a lens, due to scattering by surface irregularities, interfacial surface reflections, etc., has already been proposed.[7] Briefly, the method consists of determining the relative illumination at the centre of the image of a small, opaque, 'black' patch located as an axial object in an otherwise large and uniformly bright field. If a small 'pin-hole' aperture is placed in the plane of focus and at the centre of the image, the illumination can be determined by measuring with a photocell the light flux emerging from the 'pin hole' relative to that emerging when the 'black' patch is removed. This ratio has been termed the veiling-glare index, and is usually expressed as a percentage.

However, it was suggested to the writer, by Dr J. M. Burch of the National Physical Laboratory, that it should be possible to observe the actual sources of flare within the lens if the photocell is replaced by a lens focused on the exit pupil of the lens under examination. Thus an image of the flare-producing centres and defects on the lens surfaces may be obtained behind the pin-hole aperture screen where they may be photographed directly or observed with a simple eyepiece.

12. Method

The diagram shown in Fig. 15 (not drawn to scale) indicates the optical arrangement which was used to explore this interesting suggestion. It will be seen from the figure that only the light which has been severely scattered by reflection, refraction, or diffraction from its true geometrical transmission path (i.e. the flare-light) can be accepted by the 'pin-hole' aperture because of the focal-isolation effect. Thus the method is similar to the well-known dark-field illumination technique employed in microscopy.

The lens replacing the photocell is a low-power microscope objective. An eyepiece (not shown) is used to observe the flare-pattern and adjust the apparatus; it can then be removed and the flare-pattern imaged on to a photographic plate for recording.

It was necessary to use a larger 'pin-hole' than for the corresponding photoelectric measurement, simply because of the loss of sharpness due to diffraction. On the

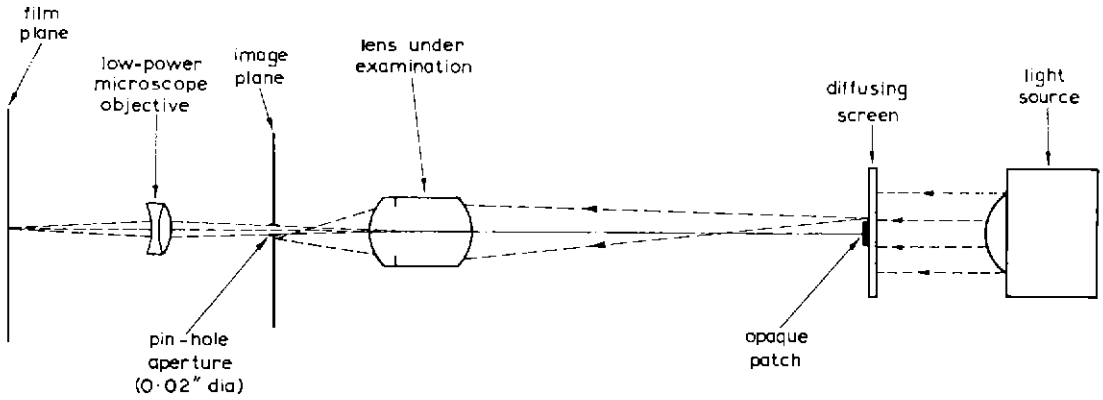

Fig. 15 — Optical arrangement

other hand, the 'pin-hole' must not be too large because a substantial depth of focus is required if the flare-centres on all the surfaces of the lens are to be observed, simultaneously, with reasonable definition. A 'pin-hole' diameter of 0·02 in. (0·51 mm) was found to be a good compromise, in conjunction with a 2 in. (51 mm) or 3 in. (76 mm) microscope objective. The focusing procedure adopted was to adjust for maximum edge-sharpness on the iris-blades.

13. Results for Several Lenses

The flare-source patterns exhibited by several lenses, some with deliberately introduced surface defects, have been recorded and are shown in Figs. 17 to 26. Fig. 16 is the ideal pattern representing a lens with zero veiling-glare index, and the plate also gives a standard of comparison for 'black' as reproduced by the lithographic process in the other photographs. Fig. 17 shows the nearest approach to the ideal so far encountered in a highly-corrected lens.

The type of lens and a brief description of the major defect responsible for each flare-pattern is appended to the photographs. Defects such as fingerprints and scratches are self-evident. In general, the predominant 'sky-at-night' type of pattern is due to dust particles on the glass/air surfaces, while the 'milky-way' type of galaxy (as in Fig. 20) is probably due to a defective antireflection coating. A grey background to the flare-centres implies no (or very inefficient) antireflection coatings on the glass/air surfaces; conversely, a dark background suggests efficient 'blooming'. Broad, smudgy, light-patches may be due to greasy organic deposits. The bright circumferential rings are due to the edges of the iris-blades.

Fig. 16 — *Ideal flare-pattern*

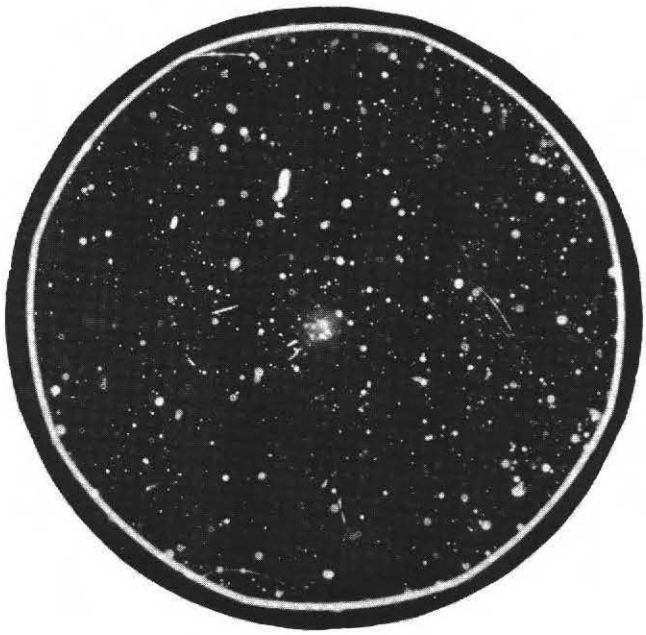

Fig. 17 — *Enlarging lens* 80 *mm f*/4·5

Veiling-glare index 0·5 *per cent. Rather bright iris-rim, but good 'blooming'. Some dust on internal surfaces*

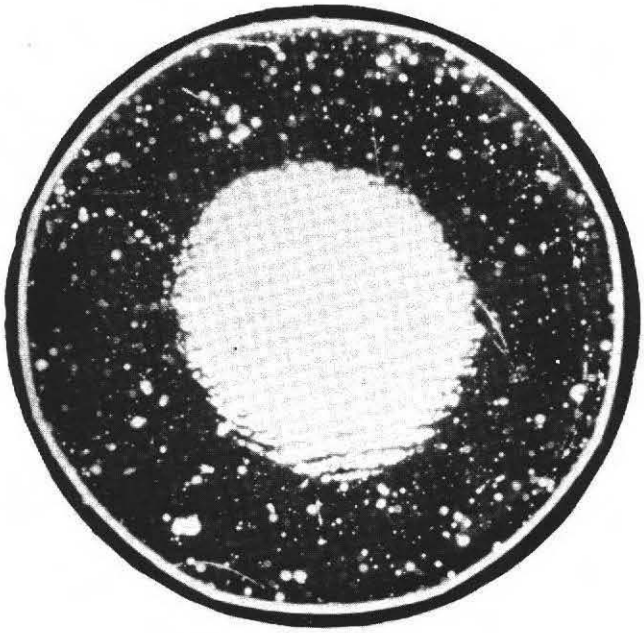

Fig. 18 — *Enlarging lens* 80 *mm f*/4·5
(*same lens as in Fig.* 17)

Smudged finger-print on front surface. Veiling-glare index now increased to 3·5 *per cent*

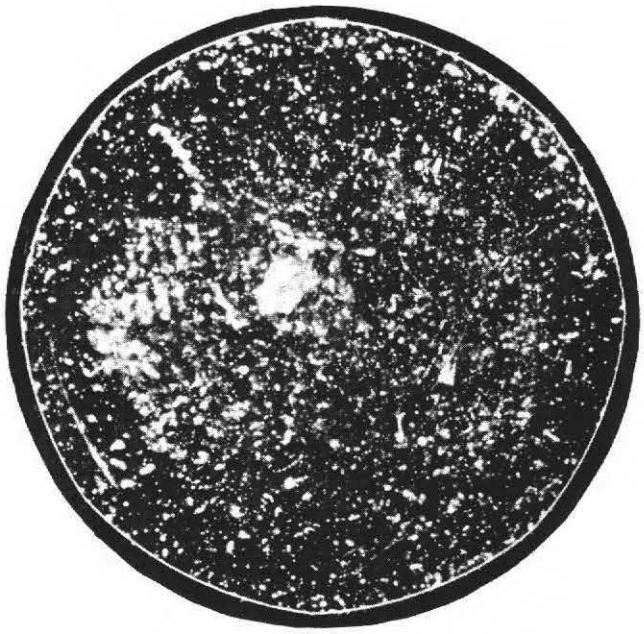

Fig. 19 — *Enlarging lens* 80 *mm f*/4·5

New lens—just unpacked—without cleaning external surfaces. Veiling-glare index 1·9 *per cent. Mainly packing-dust, slight finger-print*

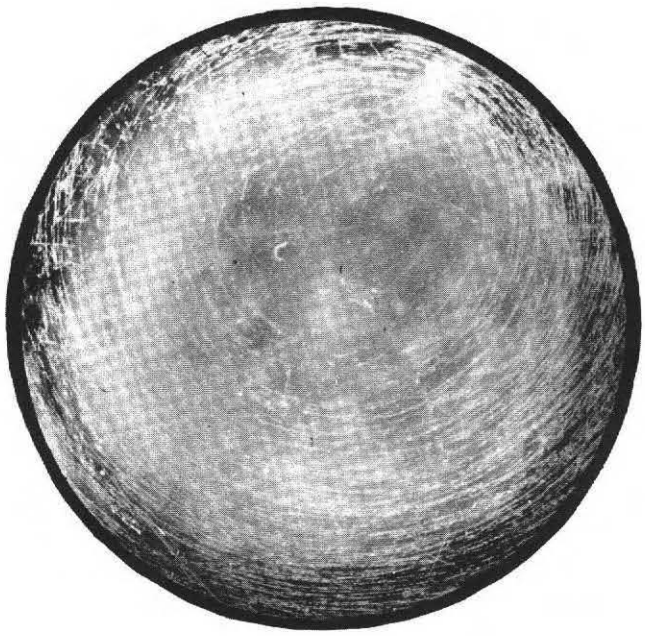

Fig. 21 — *Camera lens* 5 *cm f*/1·5

An attempt to remove a hard grimy deposit on the front surface by rubbing with dry cotton-wool. Veiling-glare index 2·3 *per cent*

Fig. 20 — *Enlarging lens* $3\frac{1}{4}$ *in. f*/4·5

Defective 'blooming' on rear surface of front element. Veiling-glare index 2·0 *per cent*

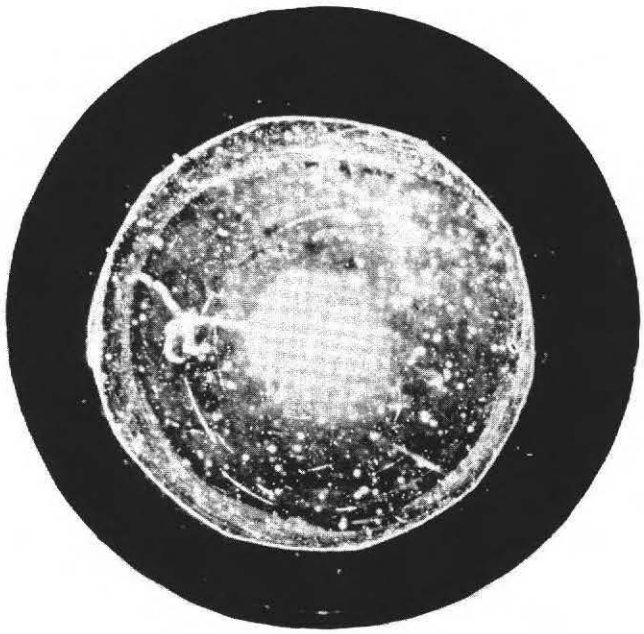

Fig. 22 — *Enlarging lens* 2 *in. f*/4·5

'Unbloomed' lens. Some scratches—rather grimy deposits. Veiling-glare index 3·4 *per cent*

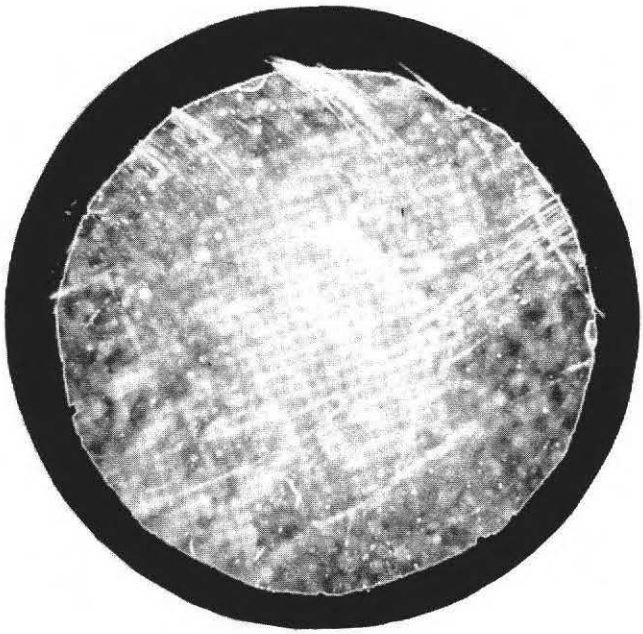

Fig. 23 — Camera lens 2 in. f/1·9

Badly scratched on several surfaces. Poor 'blooming' and some grimy deposits (note damaged iris-blades). Veiling-glare index 5·3 per cent

Fig. 25 — Enlarging lens 4 in.

Dusty internal surfaces. Good 'blooming' (black background) Veiling-glare index 2·0 per cent

Fig. 24 — Camera lens 50 mm f/3·5

Old 'unbloomed' lens. Worn and badly scratched front surface. Veiling-glare index 6·4 per cent

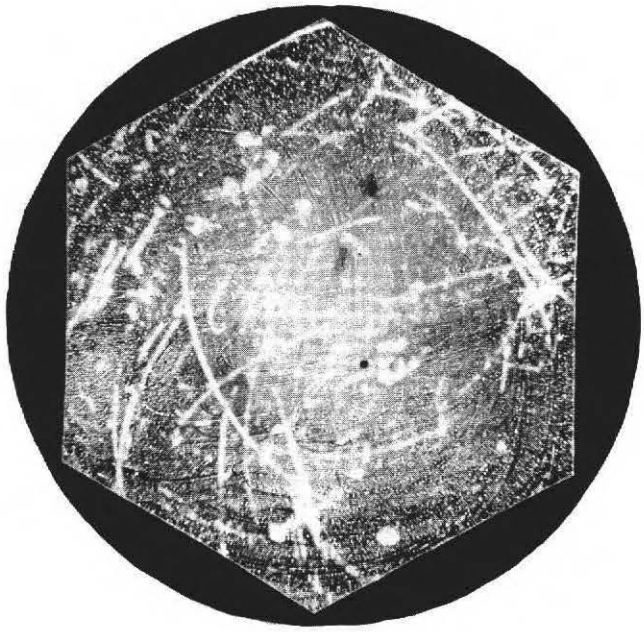

Fig. 26 — Camera lens 5 cm

'Unbloomed' lens. Deep scratches are on the front surface. Also, hard grimy deposit showing attempts to remove it with a cloth

14. Conclusions

The method affords a visual means of determining the type, location and extent of those defects of the surfaces of a lens which give rise to flare in the image plane. The results indicate that a sensitive diagnostic tool for examining ordinary camera lenses can be constructed from simple and inexpensive optical components.

An operator could rapidly acquire the experience necessary to interpret, qualitatively, the various flare-source patterns. Greater experience, supplemented in the first instance by corresponding photoelectric measurements of the veiling-glare index, would be required to establish reliable visual criteria of acceptability.

It is suggested that this type of device would be useful to those departments which deal with the general servicing of lenses.

15. Acknowledgments

The design and construction of the optical bench described in Part I were undertaken by the Precision Tool and Instrument Company. The detailed design of the scanning head and sine-wave analyser was also done by the same company working in close collaboration with the authors.

16. References

1. Sproson, W. N., **New Equipment and Methods for the Evaluation of the Performance of Lenses for Television,** BBC Engineering Monograph No. 15, December 1957.

2. Archard, T. N. J., and Rumsey, D. H., **An Optical Scanning and Recording System for a Photoelectric Optical Bench,** Electronic Engineering, Vol. 29, pp. 231–3, May 1957.

3. Sproson, W. N., **The Measurement of the Performance of Lenses,** BBC Quarterly, Vol. 8, No. 1, pp. 17–26, 1953.

4. Hacking, K., **An Optical Method of Obtaining the Frequency-Response of a Lens,** Nature, Vol. 181, pp. 1158–9, 19 April 1958.

5. Born, *et al.*, Nature, Vol. 156, 756 (1945).

6. BBC Specification for Television Lenses TV 88/2.

7. Hacking, K., **Secondary Flare in Lenses.** BBC Engineering Monograph No. 36, **Some Aspects of Optical Lens Performance,** April 1961, Part I.

APPENDIX

APERTURE CORRECTION REQUIRED BY THE SINE-WAVE ANALYSER

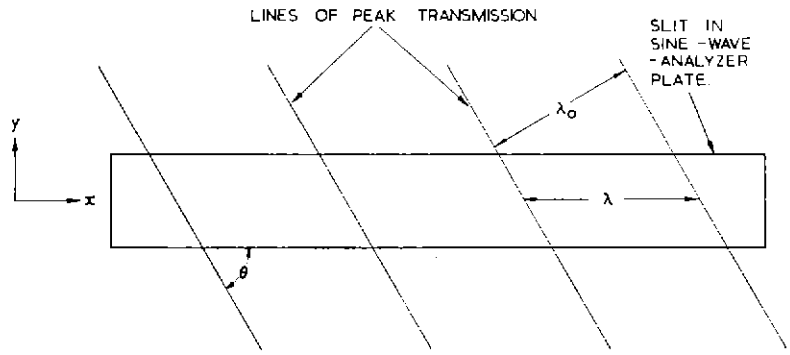

Fig. 27 — Aperture correction required by the sine-wave analyser

x=direction of independent variable of Fourier integral
y=direction of major axis of source slit

Let transmission along centre of slit be given by

$$t = A\cos(2\pi x/\lambda + \phi) + C \qquad A \leqslant C$$

where A/C = modulation

λ = effective wavelength at orientation, θ, of sine-wave plate

ϕ = arbitrary phase of grating.

At a displacement of y from centre line, the sine-wave is shifted by $-y\cot\theta$

$$\therefore\ t(y) = A\cos\left(2\pi\frac{x + y\cot\theta}{\lambda} + \phi\right) + C$$

If slit is of width $2b$, mean transmission is given by

$$\bar{t} = \frac{1}{2b}\int_{-b}^{b}\left[A\cos\left(2\pi\frac{x + y\cot\theta}{\lambda} + \phi\right) + C\right]dy$$

$$= \frac{\lambda}{2\pi b\cot\theta}\left[A\cos(2\pi x/\lambda + \phi)\sin\frac{2\pi b\cot\theta}{\lambda}\right] + C$$

Thus the original modulation A/C is multiplied by the factor

$$k = \frac{\lambda\tan\theta}{2\pi b}\sin\frac{2\pi b\cot\theta}{\lambda}$$

and this is independent of the phase angle ϕ.

This can be rewritten in terms of the effective spatial frequency $f(=1/\lambda)$ and the natural spatial frequency of the sine-wave grating $f_0(=1/\lambda_0)$

$$k = \frac{\sin\{2\pi b(f_0^2 - f^2)^{\frac{1}{2}}\}}{2\pi b(f_0^2 - f^2)^{\frac{1}{2}}}$$

Note that when $f = 0 \quad k = \dfrac{\sin 2\pi b f_0}{2\pi b f_0}$

when $f = f_0 \quad k = 1$

It will thus be seen that the variation of k with frequency is in the opposite sense to the spectrum of a thin slit.

A thin slit of width $2b$ has a spectrum proportional to

$$\frac{\sin 2\pi b f}{2\pi b f}$$

The combined effect of two slits at right angles is thus

$$\frac{\sin\{2\pi b(f_0^2 - f^2)^{\frac{1}{2}}\}}{2\pi b(f_0^2 - f^2)^{\frac{1}{2}}} \times \frac{\sin(2\pi b f)}{2\pi b f}$$

When $2b = \lambda_0/4$ the product given above is constant to about 0·1 per cent over the frequency range $f = 0$ to $f = f_0$. A narrower slit (e.g. $2b = \lambda_0/6$) does not give as good constancy of product over the range $f = 0$ to $f = f_0$ and in fact varies by about 0·5 per cent.

A Recent BBC Technical Suggestion

TWO-TUBE COLOUR CAMERA USING IMAGE ORTHICONS

The light entering the camera through a normal lens is split in two directions: (*a*) to a conventional monochrome image orthicon which provides the luminance signal (without all the problems of registration) and (*b*) to the colour image orthicon system which works as follows:

The light incoming to the colour section is split into two beams by way of two anamorphic (i.e. cylindrical) lenses. The two light beams are then passed through red and blue filters and focused side by side on to two halves of the image orthicon. Each half of the photo-cathode, therefore, has a separate image on it (coloured red and blue respectively). These images have already been 'squeezed' horizontally by the anamorphic lens to fit into the reduced aspect ratio (approximately 2:3). The scanning beam now reads off line 1 on the luminance image orthicon together with line 1 on the red half of the colour image orthicon. In the blanking period between line 1 and the next line (line 3 in the interlaced system) the image orthicon beam has been shifted bodily from the red half of the image orthicon to the blue half. Line 3 on the blue half of the colour image orthicon is now read off at the same time as line 3 in the luminance image orthicon. For line 5 the colour scanning beam is shifted back to the red half during the line 3–5 blanking period, and so on. Thus, alternate lines from the colour image orthicon are red and blue. This could be applied to a delay line system to produce an NTSC colour signal, or used for SECAM.

The signal-noise ratio of the colour image orthicon, which will be degraded by using only half the image orthicon target per line, could possibly be improved by elongating the scanning beam vertically (by spot wobble) since, in the case of, say, the red section, only lines 1 and 5 are used (line 3 comes from the blue section). The scanning beam could therefore conceivably be stretched vertically to cover lines 1, 2, 3, and 4. The mirror used to split the light into the colour and luminance sections could have its reflectance/transmission ratio adjusted to feed a proportionally larger amount of light to the colour section to compensate for lack of sensitivity in the blue. Furthermore, if the camera were constructed to use only one mirror (as illustrated) the sensitivity of the whole system could presumably be improved by comparison with the conventional three-tube image orthicon camera and its associated multiplicity of mirrors.

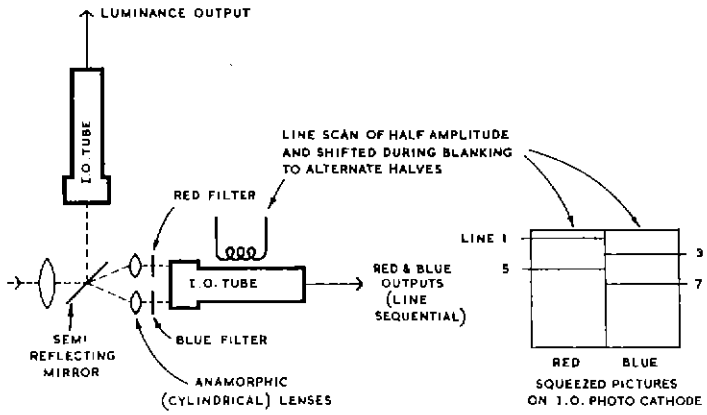

A further advantage of this camera is that under conditions of light which are too low for the colour section of the camera, it might be possible to use the output from the luminance tube to produce a conventional *monochrome* picture and, indeed, it might even be possible to remove the splitting mirror from the luminance light path if this were necessary.

J. J. BELASCO

Published by the British Broadcasting Corporation, 35 Marylebone High Street, London, W.1. Printed in England on Basingwerk Parchment in Times New Roman by The Broadwater Press Ltd, Welwyn Garden City, Herts. No. 5375